JOURNAL OF THE AMERICAN CHEMICAL SOCIETY

Communication

pubs.acs.org/JACS

Conjunction of Chirality and Slow Magnetic Relaxation in the Supramolecular Network Constructed of Crossed Cyano-Bridged $Co^{II}-W^{V}$ Molecular Chains

Szymon Chorazy,[†,‡] Koji Nakabayashi,[‡] Kenta Imoto,[‡] Jacek Mlynarski,[†] Barbara Sieklucka,*[,†] and Shin-ichi Ohkoshi*[,‡,§]

[†]Faculty of Chemistry, Jagiellonian University, Ingardena 3, 30-060 Cracow, Poland

[‡]Department of Chemistry, School of Science, The University of Tokyo, 7-3-1 Hongo, Bunkyo-ku, Tokyo 113-0033, Japan

[§]CREST, Japan Science and Technology Agency (JST), K's Gobancho, 7 Gobancho, Chidoya-ku, Tokyo 102-0076, Japan

Ⓢ *Supporting Information*

ABSTRACT: The addition of chiral 2,2′-(2,6-pyridinediyl)bis(4-isopropyl-2-oxazoline) (*i*Pr-Pybox) to a self-assembled $Co^{II}-[W^{V}(CN)_8]$ magnetic system gives two enantiomorphic cyano-bridged chains, $\{[Co^{II}((S,S)\text{-}i\text{Pr-Pybox})(MeOH)]_3[W^{V}(CN)_8]_2\cdot 5.5MeOH\cdot 0.5H_2O\}_n$ (**1**-*SS*) and $\{[Co^{II}((R,R)\text{-}i\text{Pr-Pybox})(MeOH)]_3[W^{V}(CN)_8]_2\cdot 5.5MeOH\cdot 0.5H_2O\}_n$ (**1**-*RR*). Both compounds crystallize with a structure containing a unique crossed arrangement of one-dimensional chains that form a microporous supramolecular network with large channels (14.9 Å × 15.1 Å × 15.3 Å) filled with methanol. The investigated materials exhibited optical chirality, as confirmed by natural circular dichroism and UV−vis absorption spectra. **1**-(*SS*) and **1**-(*RR*) are paramagnets with cyano-mediated $Co^{II}-W^{V}$ magnetic couplings that lead to a specific spin arrangement with half of the W^{V} ions coupled ferromagnetically with their Co^{II} neighbors and the other half coupled antiferromagnetically. Significant magnetic anisotropy with the easy axis along the [101] direction was confirmed by single-crystal magnetic studies and can be explained by the single-ion anisotropy of elongated octahedral Co^{II} sites. Below 3 K, the frequency-dependent $\chi''_M(T)$ signal indicated slow magnetic relaxation characteristic of single-chain magnets.

The introduction of required additional properties to molecular magnets is being extensively investigated, as the interaction between the intrinsic magnetic nature and new functionalities leads to extraordinary cooperative effects such as magnetochiral dichroism,[1] magnetic second-harmonic generation,[2−4] and multiferroicity[5−8] when chirality is combined with long-range magnetic ordering. Microporous magnets have also attracted enormous interest, as reversible guest exchange can significantly affect the magnetic character.[9,10]

A considerable number of enantiopure chiral and microporous magnets have been characterized.[9−14] Among them, extensive research has been devoted to cyano-bridged bimetallic assemblies, which exhibit a wide range of magnetic properties, including magnetic ordering, spin bistability, and magnetic anisotropy.[15−20] In this regard, octacyanometalates $[M^{IV/V}(CN)_8]^{4-/3-}$ (M = Nb, Mo, W) are certainly promising, as their eight coordination sites and stereochemical flexibility enhance dynamic changes during sorption processes and facilitate the construction of various chiral motifs and topologies.[4,20−26] Several two- and three-dimensional chiral and guest-responsive systems based on 3d metal ions and octacyanides have been investigated.[20−26] We have focused on the unexplored area of one-dimensional (1D) systems combining chirality, slow magnetic relaxation, and microporosity. The general synthetic methodology is to employ anisotropic metal centers and appropriate organic ligands to ensure (a) the desired dimensionality; (b) good magnetic isolation of the chains, which is essential for slow magnetic relaxation; (c) chirality; and (d) microporous character.[20] The last point is especially challenging, as 1D chains are typically arranged in parallel and solvent exchange causes their random reorientation. We overcame these difficulties by using the chiral rigid tridentate Pybox derivative 2,2′-(2,6-pyridinediyl)bis(4-isopropyl-2-oxazoline) (*i*Pr-Pybox) along with internally anisotropic Co^{II} centers and paramagnetic $[W^{V}(CN)_8]^{3-}$ ions. We report the synthesis, crystal structures, and properties of 1D bimetallic $\{[Co^{II}((S,S)\text{-}i\text{PrPybox})(MeOH)]_3[W^{V}(CN)_8]_2\cdot 5.5MeOH\cdot 0.5H_2O\}_n$ (**1**-*SS*) and $\{[Co^{II}((R,R)\text{-}i\text{Pr-Pybox})(MeOH)]_3[W^{V}(CN)_8]_2\cdot 5.5MeOH\cdot 0.5H_2O\}_n$ (**1**-*RR*) chains combining chirality with magnetic anisotropy, leading to single-chain-magnet behavior.

1-(*SS*) and **1**-(*RR*) were obtained as orange rhombic plates from mixtures of $Na_3[W^{V}(CN)_8]\cdot 4H_2O$ and $Co^{II}Cl_2\cdot 6H_2O$ with (*S*,*S*)- and (*R*,*R*)-*i*Pr-Pybox, respectively, in methanol upon the addition of diisopropyl ether. Single-crystal X-ray diffraction revealed that **1**-(*SS*) is a 1D cyano-bridged molecular polymer with 3,2-topology that crystallizes in the chiral *C*2 space group (Figure 1; also see Tables S1−S4 and Figures S1−S3 in the Supporting Information). Each chain is built from $\{[cis\text{-}Co^{II}(NC)_2]_2W^{V}_2\}$ squares connected via $\{trans\text{-}Co^{II}(NC)_2\}$ moieties. The asymmetric unit contains three Co^{II} and two $[W^{V}(CN)_8]^{3-}$ ions. Both $[W1^{V}(CN)_8]^{3-}$ and $[W2^{V}(CN)_8]^{3-}$ form three cyanide bridges each, and their geometries are between square-antiprismal (SAPR-8) and dodecahedral (DD-8) (Tables S3 and S4). All of the Co^{II} ions are six-coordinate and

Received: July 31, 2012
Published: September 18, 2012

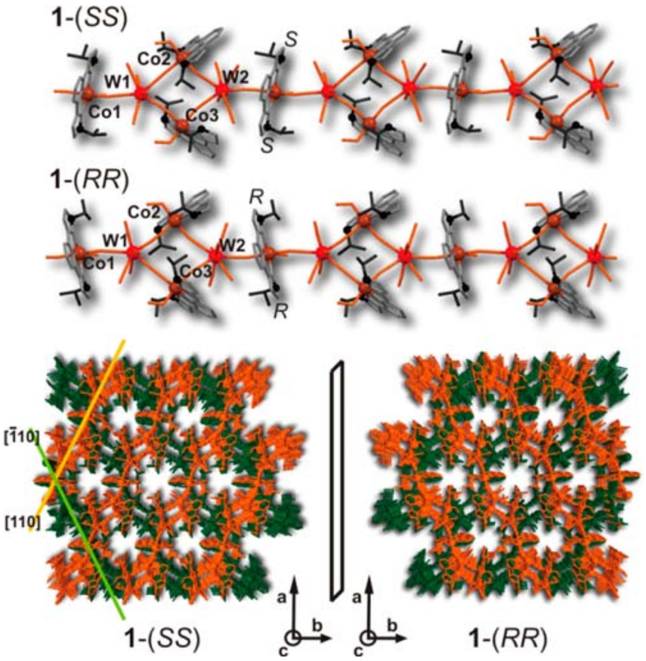

Figure 1. Crystal structures of **1**-(*SS*) and **1**-(*RR*): (top) 1D coordination polymers; (bottom) crossed arrangement of chains giving microporous networks.

adopt a distorted octahedral geometry. Co1 is coordinated with two cyanide N atoms trans to each other, three meridionally arranged Pybox N atoms, and one methanol O atom. Co2 and Co3 have similar coordination spheres but with a cis configuration of the cyanide ligands. Molecular chains of **1**-(*SS*) are arranged crosswise, as half of chains are situated in the [110] direction while the remaining ones lie along [$\bar{1}$10]. This gives a chiral porous supramolecular network with vast channels along the *c* axis (Figure 1). From the viewpoint of the W−Co skeleton, these channels have a decagonal shape limited by six Co^{II} and four W^{V} centers. Their dimensions are 15.3 Å × 15.1 Å × 14.9 Å, and the cross-sectional area is 178.1 Å^2. They are filled by weakly bonded methanol (Figure S2). The crystal structure of **1**-(*RR*) is an almost ideal structural mirror image of **1**-(*SS*) (Figure 1). The coordination skeleton, geometries of the metal centers, and size of the channels in **1**-(*RR*) are identical to those in **1**-(*SS*) (Tables S1−S4 and Figures S1−S3).

To examine the optical properties, UV−vis diffuse reflectance spectra together with natural circular dichroism (NCD) spectra were acquired (Figure 2). Besides the UV absorption, **1**-(*SS*) and **1**-(*RR*) exhibit a broad band between 400 and 700 nm with a maximum at 490 nm. Deconvolution of the spectrum gave four main components with maxima at 335 (peak 1), 465 (peak 2), 530 (peak 3), and 590 nm (peak 4). They can be assigned to ligand-to-metal charge transfer from CN$^-$ to W^{V} [E″(^{2}B$_1$) → E′(^{2}A$_2$) and E″(^{2}B$_1$) → E′(^{2}E); peak 1],[27] metal-to-metal charge transfer (Co$^{II}_{HS}$ → W^{V}; peak 2),[28] and d−d transitions in high-spin (HS) Co^{II} centers [^{4}T$_{1g}$(^{4}F) → ^{4}T$_{1g}$(^{4}P) for peak 3; ^{4}T$_{1g}$ → ^{4}A$_{2g}$ for peak 4].[29] In NCD spectra, **1**-(*SS*) exclusively shows a positive signal while **1**-(*RR*) exhibits only a negative Cotton effect (Figure 2). The shape of the NCD spectrum of **1**-(*SS*) is close to that observed in the absorption mode, and the spectrum of **1**-(*RR*) is its mirror image in relation to the baseline. These results clearly prove the enantiopure character of both compounds and show that chirality related to the ligand induces chirality in the whole structure.

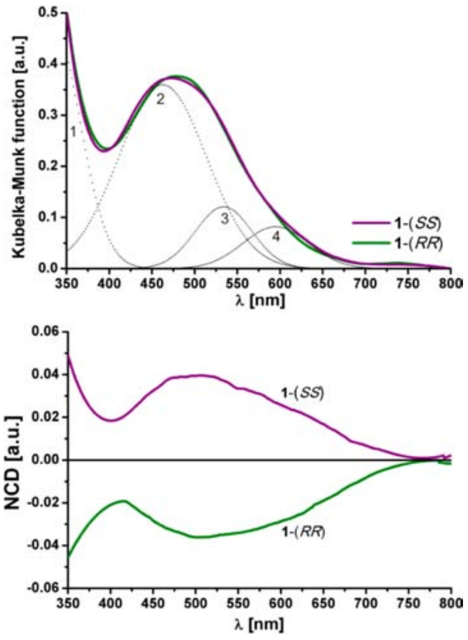

Figure 2. (top) UV−vis diffuse reflectance spectra and (bottom) NCD spectra of **1**-(*SS*) and **1**-(*RR*).

The direct-current (dc) magnetic properties of **1**-(*SS*) and **1**-(*RR*) are presented in Figure 3. The magnetic susceptibility−

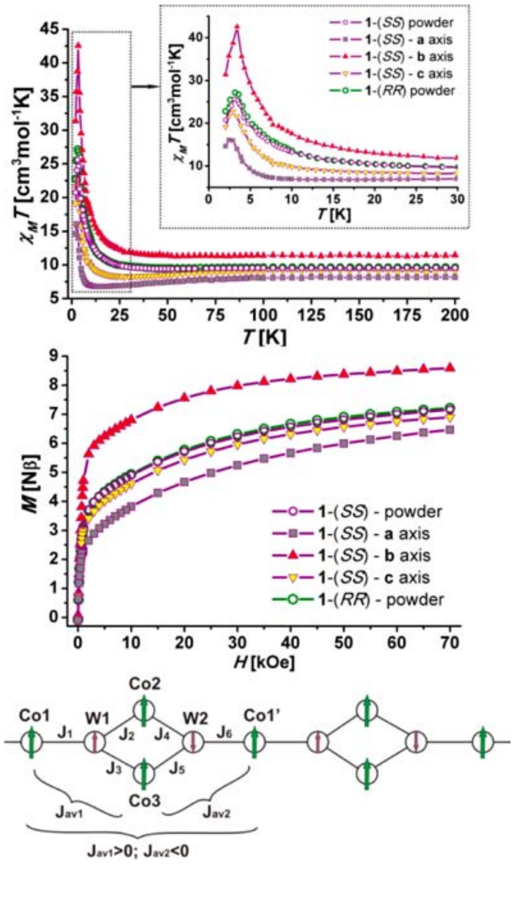

Figure 3. (top) Temperature dependence of $\chi_M T$ (H = 2 kOe). (middle) Field dependence of the magnetization (T = 2 K). (bottom) One of the two possible spin arrangements (the other possibility is shown in Figure S5).

temperature product ($\chi_M T$) at room temperature is 9.6 K cm^3 mol^{-1} (*SS* and *RR*), corresponding to uncoupled Co$^{II}_3$W$^V_2$ units ($S_W = {}^1/_2$, $g_W = 2.0$, $S_{Co_{HS}} = {}^3/_2$, $g_{Co} = 2.5$). Upon cooling, $\chi_M T$ slowly decreases, reaching a shallow minimum at ~47 K; sharply increases to a maximum of 25.6 (*SS*) or 27.1 K cm^3 mol^{-1} (*RR*) at 3.2 K as a result of Co^{II}–W^V magnetic coupling; and finally decreases because of single-ion effects of Co^{II}. The value of the magnetization (*M*) at 2 K under a magnetic field of 7 T is 7.2 $N\beta$ (*SS* and *RR*) which is situated between the expected values of 8.6 $N\beta$ for ferromagnetic and 4.6 $N\beta$ for antiferromagnetic Co$^{II}_3$W$^V_2$ units (assuming $S_W = {}^1/_2$, $g_W = 2.0$, $S_{Co,eff} = {}^1/_2$, $g_{Co,average} = {}^{13}/_3$).[30] This indicates that Co^{II}–W^V magnetic coupling leads to a specific spin arrangement with half of the W^V centers coupled ferromagnetically with Co^{II} neighbors and the other half coupled antiferromagnetically (Figure 3 bottom).[25]

Figure 3 shows plots of $\chi_M T$ versus *T* and *M* versus magnetic field (*H*) for single-crystalline **1**-(*SS*) and, for comparison, powder forms of **1**-(*SS*) and **1**-(*RR*). Over the whole temperature range, the $\chi_M T$ values for the *b* axis are greater than those for the powder sample, whereas for the *a* and *c* directions, the signals are lower. On cooling, $\chi_M T$ decreases slightly for all axes, with *c* having the most significant minimum and *b* a merely vestigial one. For the *b* axis, the magnetization reached 8.5 $N\beta$, corresponding to $g_{Co,b} = 5.6$ (assuming $S_W = {}^1/_2$, $g_W = 2.0$, $S_{Co,eff} = {}^1/_2$). For the *a* and *c* axes, the estimated *g* factors are 4.3 and 4.6, respectively. Figure 4a shows the rotation dependence of *M* measured in the *ac*, *ab*, and *bc* planes. The easy axis of magnetization was found to lie in the *ac* plane 70° from *a* going toward *c* within the obtuse angle, which corresponds to the shorter diagonal of the unit-cell wall (the [101] direction). Moreover, the hard axis was also observed to lie in the *ac* plane and cover the second diagonal (the $[10\bar{1}]$ direction) (Figure 4c). The magnetization along the easy axis saturated at 8.7 $N\beta$, giving a high g_{Co} value of 5.8, while for the hard axis, *M* reached only 3.5 $N\beta$ without saturation.

Neither the easy axis nor the hard axis is parallel or perpendicular to the chains; both axes are instead related to the arrangement of the Co^{II} moieties. On the basis of the geometrical parameters (Co–N and Co–O bond lengths and N–Co–N and N–Co–O angles; Table S2), the Co^{II} ions in **1**-(*SS*) are tetragonally deformed octahedra with the elongation along two of the Co–N$_{oxazoline}$ bonds. The angular distortion toward the pyridine rings plays a minor role (Figure 4d). The easy axis of magnetization is consistent with elongation of the axes of the Co2 and Co3 centers, while the hard axis is almost perpendicular to them (Figure 4c). Co1 is not important here, as its elongation axis is perpendicular to the *ac* plane. The rotation dependences for other planes can be similarly explained (Figure S7). Thus, the magnetic anisotropy of **1**-(*SS*) is controlled by the single-ion anisotropy of the Co^{II} ions, with the easy axis approximated by the elongation direction along the Co–N$_{oxazoline}$ bonds. Such behavior has been observed in other reported magnetic systems based on elongated octahedral Co^{II} ions.[31,32]

The field-cooled (FC) and zero-field-cooled (ZFC) *M* versus *T* curves for **1**-(*SS*) and **1**-(*RR*) do not diverge (Figure S6), indicating the absence of long-range magnetic ordering and good isolation of the molecular chains. Together with the significant anisotropy, this leads to a frequency dependence of the out-of-plane alternating-current (ac) magnetic susceptibility (χ''_M) in the lowest temperature regime, suggesting the onset of slow magnetic relaxation (Figure 5). Despite the fact maxima of χ''_M were not observed even with an applied dc magnetic field (H_{dc}), we estimated the values for the relaxation time (τ_0) and the activation energy (E_a) using plots of $\ln(\chi''_M/\chi'_M)$ versus T^{-1} (where χ'_M is the in-plane ac magnetic susceptibility), as described by Pardo and co-workers[12] (Figure 5). Obtained values ($\tau_0 = 5 \times 10^{-7}$ s, $E_a = 6$ K) suggested a single-chain magnet behavior.[12–14]

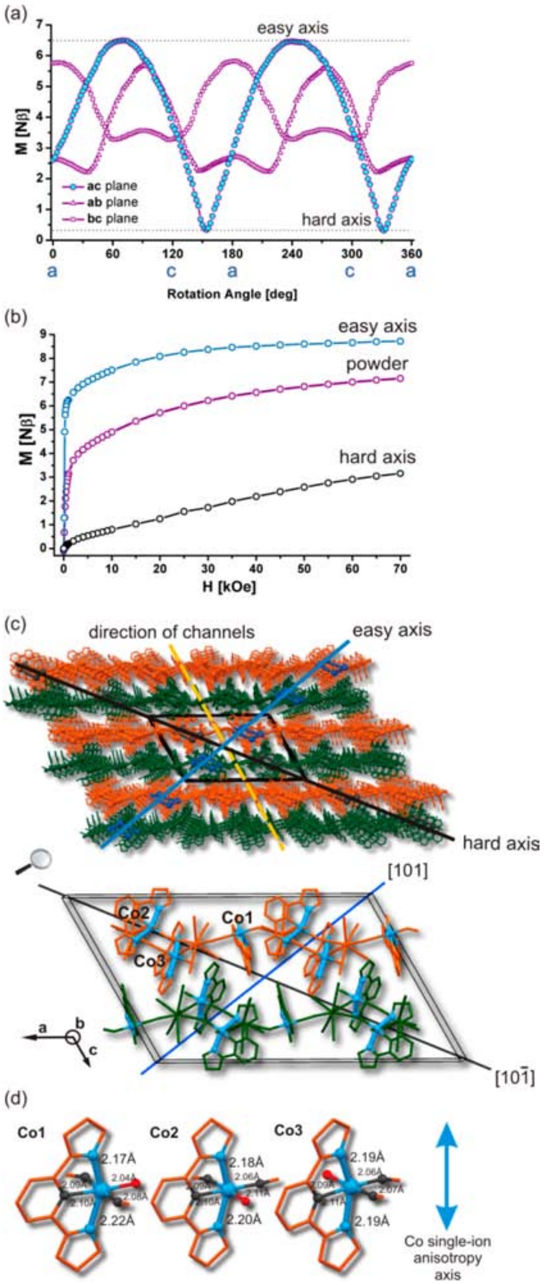

Figure 4. Magnetic properties of **1**-(*SS*): (a) rotation dependence of *M* measured in various planes ($T = 2$ K, $H = 2000$ Oe); (b) *M* vs *H* curves for the easy and hard axes; (c) arrangement of the hard and easy axes in relation to the structure; (d) geometries of the Co^{II} ions.

In summary, we have prepared two 1D cyano-bridged Co^{II}–W^V chains combining chirality and magnetic anisotropy, leading to slow magnetic relaxation. This multifunctionality is directed by an organic Pybox ligand that (1) generates the 1D topology; (2) introduces optical chirality; (3) controls the magnetic anisotropy, as the decisive elongation of the octahedral Co^{II} moieties is connected with the alignment of the Pybox rings; and (4) contributes to the slow magnetic relaxation, ensuring good magnetic isolation. The applied ligand is also responsible for the

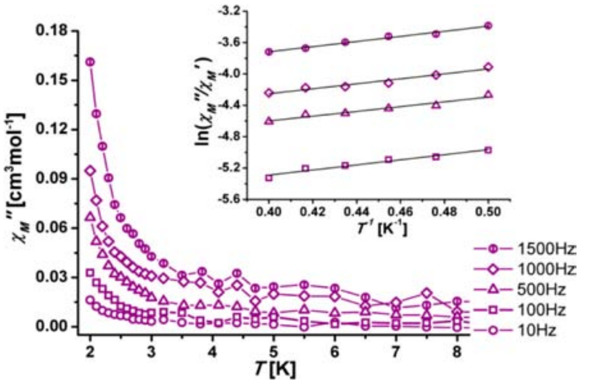

Figure 5. χ''_{M} vs T plots at $H_{\mathrm{dc}} = 0$ and (inset) $\ln(\chi''_{\mathrm{M}}/\chi'_{\mathrm{M}})$ vs T^{-1} plots for **1**-(*SS*) at various ac frequencies.

crossed arrangement of chains, giving the supramolecular network with vast channels. This last feature opens a great perspective in exploring the dynamic character of our materials, as methanol occupying the micropores can be replaced by water without loss of crystallinity (Figure S8). Research along this line is now in progress.

■ ASSOCIATED CONTENT

Ⓢ Supporting Information

Crystallographic data (CIF), details of design and synthesis, crystal data and structure refinement, structural views, results of continuous shape measure analysis and the dihedral angles method, ZFC and FC magnetization curves, detailed analysis of single-crystal magnetic data, and powder diffractograms of hydrated forms. This material is available free of charge via the Internet at http://pubs.acs.org.

■ AUTHOR INFORMATION

Corresponding Author

ohkoshi@chem.s.u-tokyo.ac.jp; barbara.sieklucka@uj.edu.pl

Notes

The authors declare no competing financial interest.

■ ACKNOWLEDGMENTS

The authors acknowledge Miguel Llunell and Santiago Alvarez for making available the SHAPE program (version 2.0) and Ms. M. Wis for executing the calculations. This work was partially supported by the International Ph.D. Studies Programme of the Faculty of Chemistry of Jagiellonian University within the Foundation for Polish Science MPD Programme, cofinanced by the EU European Regional Development Fund; the Polish National Science Centre within Research Project DEC-2011/01/B/ST5/00716; the Core Research for Evolutional Science and Technology (CREST) Program of JST; a Grant-in-Aid for Young Scientists (S) from the Japan Society for the Promotion of Science; a Grant for the Global COE Program "Chemistry Innovation through Cooperation of Science and Engineering", Advanced Photon Science Alliance (APSA), from the Ministry of Education, Culture, Sports, Science and Technology of Japan (MEXT); and the Asahi Glass Foundation. We also recognize the Cryogenic Research Center, The University of Tokyo, and the Center for Nano Lithography & Analysis of The University of Tokyo, which are supported by MEXT.

■ REFERENCES

(1) Train, C.; Gheorghe, R.; Krstic, V.; Chamoreau, L. M.; Ovanesyan, N. S.; Rikken, G.; Gruselle, M.; Verdaguer, M. *Nat. Mater.* **2008**, *7*, 729.

(2) Nuida, T.; Matsuda, T.; Tokoro, H.; Sakurai, S.; Hashimoto, K.; Ohkoshi, S. *J. Am. Chem. Soc.* **2005**, *127*, 11604.

(3) Train, C.; Nuida, T.; Gheorghe, R.; Gruselle, M.; Ohkoshi, S. *J. Am. Chem. Soc.* **2009**, *131*, 16838.

(4) Pinkowicz, D.; Podgajny, R.; Nitek, W.; Rams, M.; Majcher, A. M.; Nuida, T.; Ohkoshi, S.; Sieklucka, B. *Chem. Mater.* **2011**, *23*, 21.

(5) Spaldin, N. A.; Fiebig, M. *Science* **2005**, *309*, 391.

(6) Ohkoshi, S.; Tokoro, H.; Matsuda, T.; Takahashi, H.; Irie, H.; Hashimoto, K. *Angew. Chem., Int. Ed.* **2007**, *46*, 3238.

(7) Eerestein, W.; Mathur, N. D.; Scott, J. F. *Nature* **2006**, *442*, 759.

(8) Pardo, E.; Train, C.; Liu, H.; Chamoreau, L.-M.; Dkhil, B.; Boubekuer, H.; Lloret, F.; Nakatani, K.; Tokoro, H.; Ohkoshi, S.; Verdaguer, M. *Angew. Chem.* **2012**, *124*, 8481.

(9) Dechambenoit, P.; Long, J. R. *Chem. Soc. Rev.* **2011**, *40*, 3249.

(10) Maspoch, D.; Ruiz-Molina, D.; Veciana, J. *J. Mater. Chem.* **2004**, *14*, 2713.

(11) Train, C.; Gruselle, M.; Verdaguer, M. *Chem. Soc. Rev.* **2011**, *40*, 3297.

(12) Ferrando-Soria, J.; Cangussu, D.; Eslava, M.; Journaux, Y.; Lescouëzec, R.; Julve, M.; Lloret, F.; Pasán, J.; Ruiz-Pérez, C.; Lhotel, E.; Paulsen, C.; Pardo, E. *Chem.—Eur. J.* **2011**, *17*, 12482.

(13) Hoshino, N.; Sekine, Y.; Nihei, M.; Oshio, H. *Chem. Commun.* **2010**, *46*, 6117.

(14) Pardo, E.; Train, C.; Lescouëzec, R.; Journaux, Y.; Pasán, J.; Ruiz-Pérez, C.; Delgado, F. S.; Ruiz-Garcia, R.; Lloret, F.; Paulsen, C. *Chem. Commun.* **2010**, *46*, 2322.

(15) Ohkoshi, S.; Tokoro, H.; Hashimoto, K. *Coord. Chem. Rev.* **2005**, *249*, 1830.

(16) Lescouëzec, R.; Vaissermann, J.; Ruiz-Pérez, C.; Lloret, F.; Carrasco, R.; Julve, M.; Verdaguer, M.; Dromzee, Y.; Gatteschi, D.; Wernsdorfer, W. *Angew. Chem.* **2003**, *115*, 1521.

(17) Li, D.; Clerac, R.; Parkin, S.; Wang, G.; Yee, T.; Holmes, S. M. *Inorg. Chem.* **2006**, *45*, 5251.

(18) Harris, T. D.; Bennett, M. V.; Clerac, R.; Long, J. R. *J. Am. Chem. Soc.* **2010**, *132*, 3980.

(19) Miller, J. S. *Chem. Soc. Rev.* **2011**, *40*, 3266.

(20) Nowicka, B.; Korzeniak, T.; Stefańczyk, O.; Pinkowicz, D.; Chorazy, S.; Podgajny, R.; Sieklucka, B. *Coord. Chem. Rev.* **2012**, *256*, 1946.

(21) Tsunobuchi, Y.; Kosaka, W.; Nuida, T.; Ohkoshi, S. *CrystEngComm* **2009**, *11*, 2051.

(22) Orisaku, K. K.; Nakabayashi, K.; Ohkoshi, S. *Chem. Lett.* **2011**, *40*, 586.

(23) Pinkowicz, D.; Podgajny, R.; Gaweł, B.; Nitek, W.; Łasocha, W.; Oszajca, M.; Czapla, M.; Makarewicz, M.; Bałanda, M.; Sieklucka, B. *Angew. Chem., Int. Ed.* **2011**, *50*, 3973.

(24) Nowicka, B.; Rams, M.; Stadnicka, K.; Sieklucka, B. *Inorg. Chem.* **2007**, *46*, 8123.

(25) Imoto, K.; Takahashi, D.; Tsunobuchi, Y.; Kosaka, W.; Arai, M.; Tokoro, H.; Ohkoshi, S. *Eur. J. Inorg. Chem.* **2010**, 4079.

(26) Podgajny, R.; Chorazy, S.; Nitek, W.; Budziak, A.; Rams, M.; Gomez-Garcia, C. J.; Oszajca, M.; Łasocha, W.; Sieklucka, B. *Cryst. Growth Des.* **2011**, *11*, 3866.

(27) Isci, H.; Mason, W. R. *Inorg. Chim. Acta* **2004**, *357*, 4065.

(28) Ohkoshi, S.; Hamada, Y.; Matsuda, T.; Tsunobuchi, Y.; Tokoro, H. *Chem. Mater.* **2008**, *20*, 3048.

(29) Papánková, B.; Boča, R.; Dlháň, Ľ.; Nemec, I.; Titiš, J.; Svoboda, I.; Fuess, H. *Inorg. Chim. Acta* **2010**, *363*, 147.

(30) Lloret, F.; Julve, M.; Cano, J.; Ruiz-Garcia, R.; Pardo, E. *Inorg. Chim. Acta* **2008**, *361*, 3432.

(31) Barrios, L. A.; Ribas, J.; Aromi, G. *Inorg. Chem.* **2007**, *46*, 7154.

(32) Shvedenkov, Y.; Ikorskii, V.; Guschin, D.; Fursova, E.; Ovcharenko, V. *Polyhedron* **2001**, *20*, 1207.